

## TRANSFORMATION KINETIC OF $M_{23}C_6$ CARBIDE LATTICE PARAMETERS IN FERRITIC-MARTENSITIC P91 STEEL DURING THERMAL AGEING

MAKAREVIČIUS Vidas, BALTUŠNIKAS Arūnas, LUKOŠIŪTĖ Irena, KRIŪKIENĖ Rita,  
GRYBĖNAS Albertas

*Lithuanian Energy Institute, Kaunas, Lithuania, [Vidas.Makarevicius@lei.lt](mailto:Vidas.Makarevicius@lei.lt)*

### Abstract

Ferritic-martensitic P91 grade steel is widely used for manufacture pipes and boilers of thermal and nuclear power plants due to its high strength and creep behaviour at high temperatures and the advantage of small thermal stress in cyclic operations. During long-term operation of power plant components under elevated temperatures and steam pressure the changes of steels structure occur, on which those mechanical features and remnant service life depend. Due to diffusion processes at elevated temperatures, alloying elements replace iron within carbides, leading to precipitate and coarsening of more thermodynamically favoured alloy carbides as well as lattices parameters of those changing. Thermal ageing effect on the crystal structure parameters changes of  $M_{23}C_6$  carbide during long term thermal exposure at 600, 650 and 700 °C temperatures have been performed. The identification of alloy carbides and calculation of their lattice parameters have been accomplished by XRD analysis using the Powder Cell program based on the Le Bail pattern-decomposition method. X-ray diffraction revealed that carbide  $M_{23}C_6$  crystal lattice parameter changes as a function of time at high temperature exposure in laboratory conditions. Johnson-Mehl-Avrami (JMA) law was applied for the calculation changes of carbides activation energy  $E$ , lattice transformation rate constant  $k$ , lattice parameter  $a$  and transformation constant  $n$ .

**Keywords:** Steel P91, thermal ageing, XRD analysis, carbides, lattice parameters

### 1. INTRODUCTION

In the 1970s the P91 steel was developed for manufacturing of pipes and vessels in new Japanese and European power plants [1]. Better creep strength at high temperatures and pressure due to the addition of carbonitride forming elements such as niobium and vanadium to the base plain 9Cr-1Mo (P9) composition was derived [2]. Also this steel has high strength and low thermal expansion coefficient, so that the thickness of pipe can be reduced by comparison with the behaviour of other steels and these characteristic causes P91 to have significant advantages compared to other high temperature resistant steels [3]. Structural stability of heat resistant steel after long term service is one of the most important factors to the safety and reliability of engineering components. In order to achieve comprehensive information on the steel structural stability, experimental and theoretical methods are often combined. Latest computer software was used for creep-life, fatigue-life, and creep/fatigue-life calculations. Microstructure characterization methods together with thermodynamic and kinetic modelling provided comprehensive information about long-term microstructure stability of the ferritic-martensitic steels [4]. Thermo-kinetic simulation of precipitate evolution during operation of heat-resistant power plant steels (P91 and P92) was carried out using MatCalc software, Gibbs energy database and a mobility database for steels. MX and  $M_{23}C_6$  were predicted to remain as major precipitates during long-term thermal exposure in these steels [5].

Due to diffusion processes at high working temperature microstructural changes takes place leading to deterioration in strength which mainly depend on the coarsening of  $M_{23}C_6$  precipitates. It was determined that the diameter of  $M_{23}C_6$  carbides increased from 100 nm in the as received steel to about 250 nm after exposure at 600 °C for 60000 h [6,7]. Chemical composition of the  $M_{23}C_6$  phase during steel operation has changed and alloying element prevails in the lattice of carbide [8] so more thermodynamically stable carbides precipitate.

Previously authors of this manuscript has shown that the lattice parameter  $a$  of carbide  $M_{23}C_6$  in low alloy steel 12X1MΦ continuously increases during steel service time. It was suggested that this structural parameter could be useful indicator of real service exposure of 12X1MΦ steel [9].

In this study with the purpose to obtain more detailed information about microstructural evolution of high alloy steel, the effect of thermal aging on the structural changes of carbide precipitates of steel P91 was investigated after long-term thermal exposure at 600, 650 and 700 °C temperatures. In order to obtain necessary data for evaluation of steel operation state the identification of carbides and calculation of their lattice parameter changes have been performed using XRD analysis and structural parameters refining programs. The evolution of the transformed carbides  $M_{23}C_6$  was described by using the Johnson-Mehl-Avrami (JMA) law, which is the most commonly used model for characterization of transformations kinetics. This research may find application for evaluation of steel condition and remnant life assessment.

## 2. EXPERIMENTAL

Heat and creep resistant ferritic-martensitic P91 steel [10] samples (20x10x10 mm) were used for thermal ageing at 600, 650 and 700 °C temperatures. Samples of P91 steel were aged in the electric furnace SNOL 7.2/1300, in which temperature is automatically was maintained with an accuracy  $\pm 1$  °C. Chemical composition of the investigated steel is presented in **Table 1**.

**Table 1** Chemical composition of the investigated P91 steel (wt.%)

Cr	V	Mo	Ni	Mn	Al	N	C	Si	Nb	P	S
8.78	0.18	0.96	0.16	0.35	0.01	0.035	0.09	0.38	0.08	0.006	<0.0005

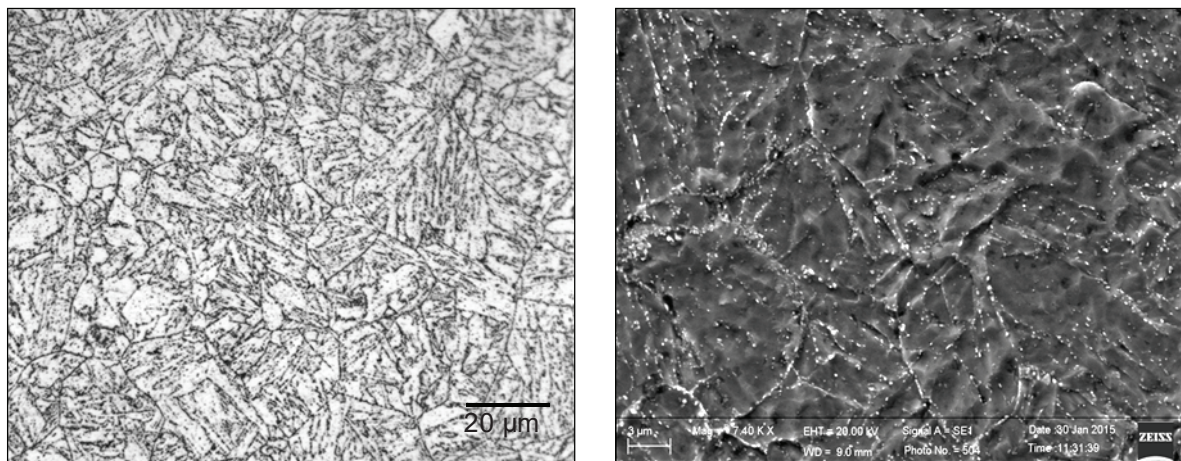


**Fig. 1** The optical microscopy (left) and scanning electron microscopy SEM (right) images of P91 steel

Microstructures of samples surface were analyzed by an optical also a scanning electron microscope. In order to highlight the steel microstructure, the polished surface was etched by Vilella's reagent. Plates of martensite, together with a large number of carbides, are observed in the SEM image of P91 steel (**Fig. 1**). The carbides are located along austenite grain boundaries.

Electrochemical extraction method was used to extract carbides from the steel. Samples were etched in 5 % hydrochloric acid solution at 130 -150 mA/cm<sup>2</sup> current densities for 8 - 10 hours. Carbides powder extracted from the steel were collected on the bottom of the flask, several times washed with warm water and dried during 24 h at 80 °C temperature. The XRD analysis of carbides from the as received and from the thermally treated steel samples was performed on the Bruker D8 Advance diffractometer, operating at the tube voltage of 40 kV and tube current of 40 mA. The X-ray beam was filtered with Ni 0.02 mm filter to select the  $CuK_{\alpha}$

wavelength. Diffraction patterns were recorded in a Bragg-Brentano geometry using a fast counting detector Bruker LynxEye based on silicon strip technology. The specimens of carbides were scanned over the range  $2\theta = 25-100^\circ$  at a scanning speed of  $1.7^\circ \text{ min}^{-1}$  using a coupled two theta/theta scan type. Silicon powder standard prepared from single crystal was added for zero shift of X-ray line determination. The data were fitted with the Powder Cell [11] programs based on the Le Bail pattern-decomposition [12] method. The XRD data on transformation kinetics of P91 steel  $M_{23}C_6$  carbide lattice parameter  $a$  was analyzed using classical Johnson-Mehl-Avrami (JMA) equation for isothermal conditions [13]:

$$x(t) = 1 - \exp[-(kt)^n], \quad (1)$$

where  $x(t)$  is the change of lattice parameter  $a$  at time  $t$ ,  $k$  is the lattice transformation rate constant,  $t$  is the time, and  $n$  is transformation constant.

In this paper the JMA equation describes how solids transform from one phase to another at constant temperature. It can specifically describe the kinetics of crystallization, but can also be applied generally to other phase changes of materials, like chemical reactions. Equation (1) can be transformed as follows [14]:

$$\ln[-\ln(1-x(t))] = n \ln k + n \ln t \quad (2)$$

$k$  and  $n$  can be found from intercept and slope of the line plotted in the form of  $\ln[-\ln(1-x(t))]$  vs  $\ln t$  respectively (the intercept is equal to  $\ln k$ ). The plot of  $\ln k$  versus  $1/T$  gives an activation energy  $E$ .

### 3. RESULTS AND DISCUSSION

The example of phase identification of XRD powder pattern of electrochemically extracted carbides from P91 steel is presented in **Fig. 2**. The XRD analysis revealed the presence of Cr-rich carbide  $M_{23}C_6$  as a main phase and also V-rich and Nb-rich  $M(C, N)$  carbo-nitrides- as minor phases in the initial as well as in the aged at elevated temperatures P91 steel. The Le Bail whole X-ray diffraction pattern profile fitting have been performed for purpose to measure precise lattice parameter  $a$  of carbide  $M_{23}C_6$ .

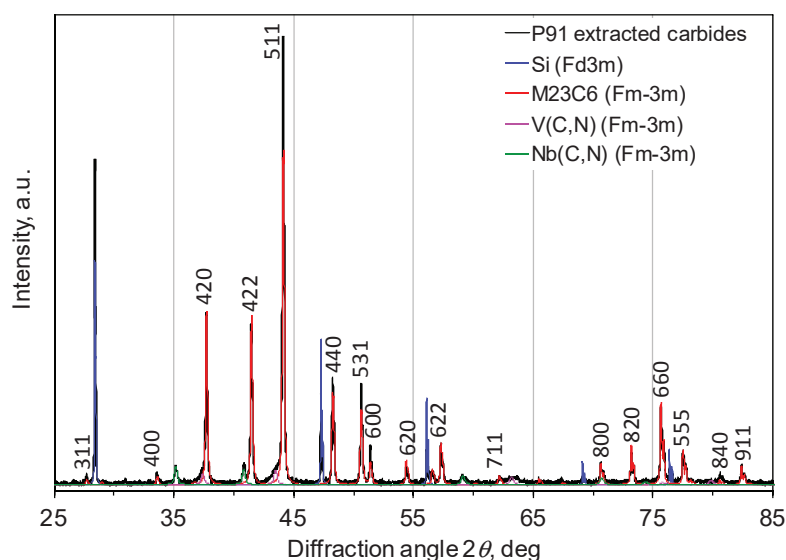


**Fig. 2** Phase identification of XRD powder pattern and carbide  $M_{23}C_6$  lattice parameter calculation using Powder Cell program and Le Bail structureless whole X-ray diffraction pattern profile fitting. Silicon powder standard prepared from single crystal was added for zero shift of X-ray line determination (Miller indices are shown only for  $M_{23}C_6$  phase)

The example of carbide  $M_{23}C_6$  Bragg peak (511) shift to lower diffraction angles after ageing P91 steel at elevated temperatures is shown in **Fig. 3**. The inset of the expanded view between  $43.8$  and  $44.8^\circ$  of  $2\theta$ , illustrates that the lattice parameter  $a$  value of cubic (space group Fm-3m) carbide  $M_{23}C_6$  depends on magnitude of ageing temperature.

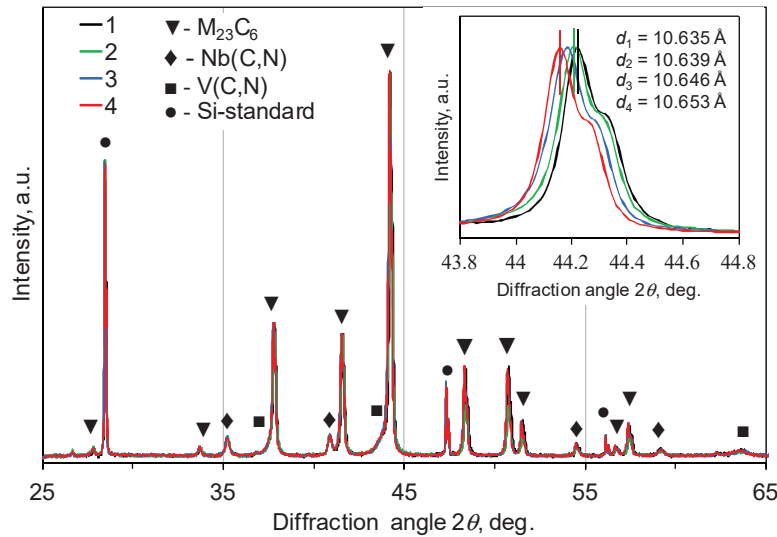


**Fig. 3** X-ray diffraction patterns of P91 steel carbides. Curves: 1 - reference, 2 - thermal treated for 42 days at  $600^\circ\text{C}$ , 3 -  $650^\circ\text{C}$  and 4 -  $700^\circ\text{C}$

The results of carbide  $M_{23}C_6$  lattice parameters measurements are summarised in **Fig. 4**, which indicates that the value of parameter  $a$  increases with increasing of temperature as well as with increasing of ageing time duration (**Fig. 4**, curves 1-3). The  $M_{23}C_6$  parameter  $a$  value changes from  $10.635\text{ \AA}$  in reference steel to  $10.653\text{ \AA}$  in steel thermally aged at  $700^\circ\text{C}$  for 42 days due to diffusion of alloying elements in the lattice of carbide [15]. During this process Fe atoms in carbide lattice were partly changed by Cr and Mo, but as diffusion coefficient of Cr is higher than Mo, consequently Cr atoms dominate in the  $M_{23}C_6$  lattice [16].

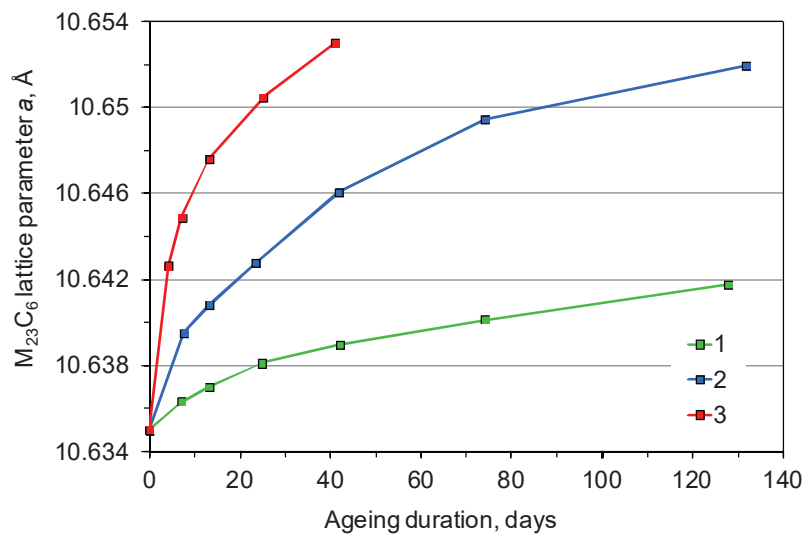


**Fig. 4** The changes of lattice parameter  $a$  of P91 steel carbide  $M_{23}C_6$  depending on ageing time at a temperature: 1 -  $600^\circ\text{C}$ , 2 -  $650^\circ\text{C}$  and 3 -  $700^\circ\text{C}$

The function of  $\ln[-\ln(a_0/a_t)]$  was evaluated as a function of  $\ln t$  (**Fig. 5**). Plots of  $\ln[-\ln(a_0/a_t)]$  vs  $\ln t$ , as shown in **Fig. 5**, yield the values of  $n$  and  $k$  for the changes of lattice parameter  $a$  of  $M_{23}C_6$  carbide at three temperatures. At all the temperatures, the plots exhibited linear dependences (**Fig. 5**, curves 1-3) hence the transformation conforms Johnson-Mehl-Avrami equation.

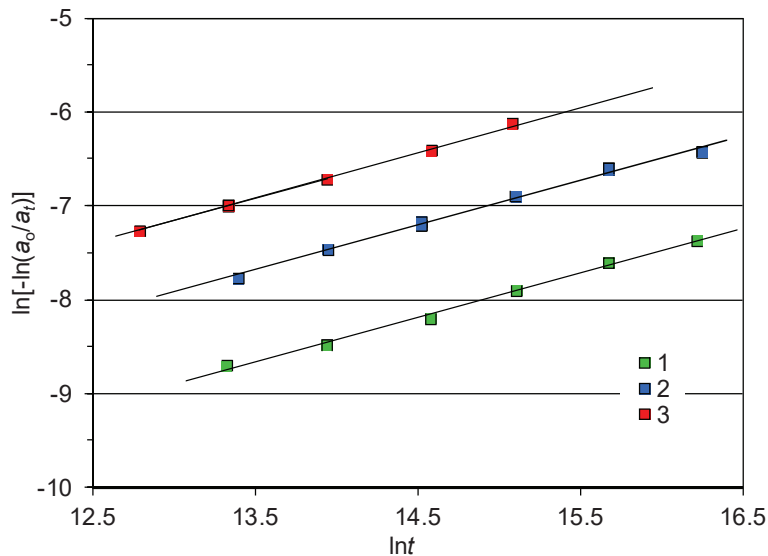


**Fig. 5** A plot between  $\ln[-\ln(a_0/a_t)]$  versus  $\ln t$  following the JMA equation in the isothermal temperature: 1 - 600 °C, 2 - 650 °C, 3 - 700 °C

The obtained equations from the linear regression adjustment are:

$$y_{600} = 0.47 \ln t - 153.08, R^2 = 0.99$$

$$y_{650} = 0.47 \ln t - 14.07, R^2 = 0.99$$

$$y_{700} = 0.48 \ln t - 13.39, R^2 = 0.99$$

where  $y = \ln[-\ln(a_0/a_t)]$ .

The linear equations (**Fig. 5**, curves 1 - 3) give values of carbide  $M_{23}C_6$  lattice parameters transformation rate constant  $k$  and the transformation constant  $n = 0.47 \div 0.48$  (**Table 2**) for all experimental temperatures have been obtained from the slope of those lines.

**Table 2** Kinetic parameters of carbide  $M_{23}C_6$  cubic lattice

$T, ^\circ\text{C}$	$n$	$\ln k$	$k$	$E, \text{kJ/mol}$
600	0.47	-31.74	$1.64 \cdot 10^{-14}$	263.5
650	0.47	-29.70	$1.27 \cdot 10^{-13}$	
700	0.48	-27.92	$7.49 \cdot 10^{-13}$	

It appears that  $n$  can be considered practically to be independent of temperature because characterize the same, i.e. diffusion process in solid media. The increment of transformation rate constant with temperature was established (**Table 2**). Activation energy of 263.5 kJ/mol presumably associated with diffusion of alloying elements in lattice of  $M_{23}C_6$  carbide in the temperature range of 600-700 °C was calculated.

#### 4. CONCLUSIONS

Electrochemically extracted carbides from P91 steel in as-received as well as in the exposed at 600, 650 and 700 °C conditions were characterized by quantitative XRD analysis.  $M_{23}C_6$  carbide rich in Cr as a main phase and carbonitrides  $M(\text{C}, \text{N})$  rich in V and Nb as a minor phase were identified in P91 steel precipitates.

Using Si standard and Le Bail structureless whole X-ray diffraction pattern profile fitting a regularly increase of crystal lattice parameter  $a$  of  $M_{23}C_6$  carbide depending on the aging time and temperature was determined. It was found that linear relationship exists between natural logarithm of aging time of steel in high temperature and the natural logarithm of crystal lattice parameter  $a$  of  $M_{23}C_6$  carbide. This relationship enabled to apply Johnson-Mehl-Avrami equation for calculation of carbide  $M_{23}C_6$  transformation kinetics parameters. Calculated transformation constant  $n = 0.47 \sim 0.48$  and activation energy  $E = 263.5$  kJ/mol indicates about diffusion character of transformation mechanism.

Obtained results could be useful for evaluation of steel P91 actual operation time and remnant life prediction.

## ACKNOWLEDGEMENTS

*This research was funded by a grant (No. MIP-023/2014) from the Research Council of Lithuania.*

## REFERENCES

- [1] MASUYAMA F. History of power plants and progress in heat resistant steels. ISIJ International, Vol. 41, 2001, pp. 612-625.
- [2] SIREESHA M., ALBERT S.K., SUNDARESAN S. Microstructure and mechanical properties of weld fusion zones in modified 9Cr-1Mo steel. Journal of Materials Engineering and Performance, Vol. 10, No. 3, 2001, pp. 320-330.
- [3] ENNIS P.J., CZYRSKA-FILEMONOWICZ A. Recent advances in creep-resistant steels for power plant application. From Sadhana - Academy Proceedings in Engineering Sciences, Vol. 28, No. 3-4, 2003, pp. 709-730.
- [4] HALD J. Microstructure and long-term creep properties of 9-12% Cr steels. International Journal of Pressure Vessels and Piping, Vol. 85, 2008, pp. 30-37.
- [5] SRINIVAS PRASAD, B.S., RAJKUMAR V.B., HARI KUMAR K.C., CALPHAD J. Computer Coupling of Phase Diagrams and Thermochemistry, Vol. 36, 2012, pp. 1-7.
- [6] PANAIT C.G., ZIELIN'SKA-LIPIEC A., KOZIEL T., CZYRSKA-FILEMONOWICZ A., GOURGUES-LORENZON A-F., BENDICK W. Evolution of dislocation density, size of subgrains and MX-type precipitates in a P91 steel during creep and during thermal ageing at 600 °C for more than 100000 h. Materials Science and Engineering A, Vol. 527, 2010, pp. 4062-4067.
- [7] SPIGARELLI S. Microstructure-based assessment of creep rupture strength in 9Cr steels. International Journal of Pressure Vessels and Piping, Vol. 101, 2013, pp. 64-71.
- [8] ZAVALETA GUTIERREZ N., DE CICCIO H., MARRERO J., DANON C.A., LUPPO M.I. Evolution of precipitated phases during prolonged tempering in a 9%Cr1%MoVNb ferritic-martensitic steel: Influence on creep performance. Materials Science and Engineering A, Vol. 528, 2011, pp. 4019-4029.
- [9] BALTUŠNIKAS A., LEVINSKAS R., LUKOŠIŪTĖ I. Analysis of heat resistant steel state by changes of lattices parameters of carbide phases Materials science (Medžiagotyra), Vol. 14, No. 3, 2008, pp.210-214.
- [10] Material data sheet P91/T91, 10/2011. ThyssenKrupp Materials International, 2011, No. 10, 3 p.
- [11] KRAUS W., NOLZE G. Powder Cell for Windows. Version 2.4. Federal Institute for Materials Research and Testing, Berlin. <http://www.ccp14.ac.uk/tutorial/powdcell/index.html>, 2008-05-26.
- [12] LE BAIL A., DUROY H., FOURQUET J.L. Ab-Initio structure determination of  $LiSbWO_6$  by X-Ray powder diffraction. Materials Research Bulletin, No. 23, 1988, pp. 447-452.
- [13] LOPES Elaine C.N., DOS ANJOS Fernanda S.C., VIEIRA Eunice F.S., CESTARI A.R. An alternative Avrami equation to evaluate kinetic parameters of the interaction of Hg (II) with thin chitosan membranes. Journal of Colloid and Interface Science, Vol. 263, 2003, pp. 542-547.
- [14] NAZARIN A., SANJAYAN J.G. Johnson-Mehl-Avrami-Kolmogorov equation for prediction of compressive strength evolution of geopolymer. Ceramics International, Vol. 41, 2015, pp. 3301-3304.
- [15] BHADESHIA H.K.D.H, HONEYCOMBE R.W.K. Steels. Microstructure and properties. 3. ed., Elsevier Ltd., 2006. 360 p.
- [16] YAMASAKI, S. Modelling Precipitation of Carbides in Martensitic Steels. University of Cambridge, 2004. 193 p.